Original Article
Metabolic Risk/Epidemiology

Diabetes Metab J 2021;45:739-752
https://doi.org/10.4093/dmj.2020.0137
pISSN 2233-6079 · eISSN 2233-6087

dmj
DIABETES & METABOLISM JOURNAL

Magnetic Resonance-Based Assessments Better Capture Pathophysiologic Profiles and Progression in Nonalcoholic Fatty Liver Disease

Seung Joon Choi[1,*], Seong Min Kim[2,*], Yun Soo Kim[3], Oh Sang Kwon[3], Seung Kak Shin[3], Kyoung Kon Kim[4], Kiyoung Lee[5], Ie Byung Park[5], Cheol Soo Choi[5], Dong Hae Chung[6], Jaehun Jung[7], MunYoung Paek[8], Dae Ho Lee[5]

Departments of [1]Radiology, [2]Surgery, Gachon University Gil Medical Center, Gachon University College of Medicine, Incheon,
[3]Division of Gastroenterology and Hepatology, Department of Internal Medicine, Gachon University Gil Medical Center, Gachon University College of Medicine, Incheon,
Departments of [4]Family Medicine, [5]Internal Medicine, [6]Pathology, [7]Preventive Medicine, Gachon University Gil Medical Center, Gachon University College of Medicine, Incheon,
[8]Siemens Healthineers Ltd., Seoul, Korea

Background: Several noninvasive tools are available for the assessment of nonalcoholic fatty liver disease (NAFLD) including clinical and blood biomarkers, transient elastography (TE), and magnetic resonance imaging (MRI) techniques, such as proton density fat fraction (MRI-PDFF) and magnetic resonance elastography (MRE). In the present study, we aimed to evaluate whether magnetic resonance (MR)-based examinations better discriminate the pathophysiologic features and fibrosis progression in NAFLD than other noninvasive methods.
Methods: A total of 133 subjects (31 healthy volunteers and 102 patients with NAFLD) were subjected to clinical and noninvasive NAFLD evaluation, with additional liver biopsy in some patients ($n=54$).
Results: MRI-PDFF correlated far better with hepatic fat measured by MR spectroscopy ($r=0.978$, $P<0.001$) than with the TE controlled attenuation parameter (CAP) ($r=0.727$, $P<0.001$). In addition, MRI-PDFF showed stronger correlations with various pathophysiologic parameters for cellular injury, glucose and lipid metabolism, and inflammation, than the TE-CAP. The MRI-PDFF and TE-CAP cutoff levels associated with abnormal elevation of serum alanine aminotransferase were 9.9% and 270 dB/m, respectively. The MRE liver stiffness measurement (LSM) showed stronger correlations with liver enzymes, platelets, complement component 3, several clinical fibrosis scores, and the enhanced liver fibrosis (ELF) score than the TE-LSM. In an analysis of only biopsied patients, MRE performed better in discriminating advanced fibrosis with a cutoff value of 3.9 kPa than the TE (cutoff 8.1 kPa) and ELF test (cutoff 9.2 kPa).
Conclusion: Our results suggest that MRI-based assessment of NAFLD is the best non-invasive tool that captures the histologic, pathophysiologic and metabolic features of the disease.

Keywords: Elasticity imaging techniques; Magnetic resonance imaging; Non-alcoholic fatty liver disease

INTRODUCTION

Nonalcoholic fatty liver disease (NAFLD) afflicts approximately 20% to 40% of the general population worldwide and is the most common cause of chronic liver disease [1,2]. The prevalence of NAFLD is consistently increasing and is particularly high in patients with type 2 diabetes mellitus or morbid obesity with a range from 50% to 60% to more than 95% depending on the study population [1,3]. Depending on the study protocols, 2/3 or more and at least 1/3 of biopsied patients with

Corresponding author: Dae Ho Lee https://orcid.org/0000-0002-8832-3052
Department of Internal Medicine, Gachon University Gil Medical Center, Gachon University College of Medicine, 21 Namdong-daero 774beon-gil, Namdong-gu, Incheon 21565, Korea
E-mail: drhormone@naver.com

*Seung Joon Choi and Seong Min Kim contributed equally to this study as first authors.

Received: Jun. 17, 2020; Accepted: Jul. 31, 2020

NAFLD have been shown to have nonalcoholic steatohepatitis (NASH) and fibrosis, respectively [1]. Additionally, NAFLD is associated with higher mortality due to cardiovascular disease, hepatocellular carcinoma (HCC), and liver diseases and thus requires surveillance for its progression, the development of related diseases, and their complications [2,4]. In particular, the presence of fibrosis and its stages are strong independent predictors of disease-specific and all-cause mortality in patients with NAFLD [5,6].

Although a liver biopsy is considered the gold standard for the assessment of NAFLD progression, this technique has inherent limitations, including severe discomfort, complications, sampling errors, and significant heterogeneity between samples [7]. Furthermore, performing liver biopsy in all patients with NAFLD with suspected progression is impractical due to the high prevalence of NAFLD.

Noninvasive imaging and blood markers have been intensively studied for the assessment of NAFLD. Transient elastography (TE) and magnetic resonance imaging (MRI) are reasonable alternative tools for the assessment of both steatosis and fibrosis in NAFLD. TE is an ultrasound-based imaging modality that allows simple, rapid, and bedside liver stiffness measurement (LSM) and controlled attenuation parameter (CAP) measurement [8]. TE-based LSM is correlated with the fibrosis stage, particularly for the severe stage of fibrosis, and CAP allows assessment of hepatic steatosis [9]. However, TE may have a significant technical failure rate for obese patients with a high body mass index (BMI) and cover limited liver areas [10]. The MRI-estimated proton density fat fraction (MRI-PDFF) can provide fast, accurate, and generalized hepatic fat measurements for the entire liver, thereby overcoming the heterogeneity of fat deposition, where magnetic resonance elastography (MRE) is a useful diagnostic tool for differentiation of histologic-determined advanced liver fibrosis from non-advanced fibrosis [11]. Recently, spin echo echo-planar imaging (EPI)–based MRE has shown a high diagnostic performance for staging liver fibrosis compared with that of gradient-recalled echo MRE sequence [12]. In addition, MRI-PDFF and MRE can be integrated into more comprehensive magnetic resonance (MR)-based examinations, including morphologic and perfusion imaging for the detection of HCC, measurement of the abdominal fat content, proton magnetic resonance spectroscopy (^{1}H-MRS), and other functional protocols, if required. Previous studies showed that MRI-PDFF and MRE were better for evaluation and follow-up of hepatic steatosis and fibrosis than TE [13]. MRI-PDFF and MRE have also been used to evaluate therapeutic outcomes in randomized clinical trials of pharmacologic agents in NAFLD and have proven to be useful and reliable [14-16]. In addition to imaging studies, clinical scoring systems and blood markers of apoptosis (e.g., the M30 fragment of cytokeratin 18 [CK-18]) or matrix turnover and fibrosis (e.g., the enhanced liver fibrosis [ELF] test) have been used as noninvasive tools [17].

However, previous studies of noninvasive tools, including TE, MRI, and the ELF test, have focused mainly on mechanical measures of liver stiffness and their correlations with the histologic grade of hepatic fibrosis [17,18]. Thus, to be more generally applicable to patients with NAFLD with various metabolic backgrounds, the mechanical and functional aspects of the imaging parameters need to be evaluated in relation to the metabolic and pathophysiologic profiles of patients with NAFLD. Furthermore, few studies have compared MRE, TE, and the ELF test simultaneously for the evaluation of fibrosis stage in NAFLD [16].

In the present study, we aimed to evaluate whether MR-based examinations better reflected the pathophysiologic features and fibrosis progression in NAFLD and to compare the methods with other noninvasive tools in the differentiation of advanced fibrosis, including clinical scoring systems, the ELF test, and TE.

METHODS

Study subjects

Between June 2017 and May 2020, a total of 133 subjects who were either healthy volunteers or patients with NAFLD were recruited from advertisements, as well as from the diabetes and endocrinology, hepatology, metabolic surgery, and health examination centers in the hospital. Study protocols were in accordance with the Declaration of Helsinki and were approved by the Institutional Review Board at the Gachon University Gil Medical Center (GAIRB2017-001, -200, and -310). All participants provided written informed consent and the studies were registered at https://cris.nih.go.kr (registration numbers KCT0005161, KCT0003144, and KCT0003527) in accordance with the World Health Organization International Clinical Trials Registry Platform.

The inclusion criteria were as follows: healthy volunteers or subjects who were diagnosed to have or suspected of having NAFLD (aged from 19 to 70 years). Additionally, we tried to

enroll subjects with evidence of NAFLD on a liver biopsy performed within 3 months prior to enrollment at a hepatology clinic of the hospital. All biopsied patients reported no significant changes in body weight or interventions for the treatment of NAFLD or comorbidities between the date of the liver biopsy and enrollment. Patients were excluded if they had excessive alcohol consumption (alcohol intake >20 g/day for women and >30 g/day for men), evidence of another coexistent liver or biliary disease (positive hepatitis B surface antigen, anti-hepatitis C virus antibody, autoimmune hepatitis, histological evidence of other concomitant chronic liver diseases, primary biliary cirrhosis, or primary sclerosing cholangitis), use of medications known to cause secondary hepatic steatosis (corticosteroids, tamoxifen, amiodarone, or methotrexate) within 1 year, drug abuse, human immunodeficiency viral infection, contraindications for MRI, including the presence of a cardiac pacemaker or other electronic implant devices, a pregnant status, or any conditions that might affect the patient competence or participation as determined by the opinion of the principal investigator.

Clinical and laboratory evaluation

A wide array of demographic, lifestyle, anthropometric, and clinical characteristics were collected, including age, sex, body weight, waist circumference (WC) and comorbidities such as hypertension and diabetes. After an overnight fast, blood sample analyses for various markers and routine biochemical tests, which included aspartate aminotransferase (AST), alanine aminotransferase (ALT), glucose, insulin, a complete blood count with a platelet count, alkaline phosphatase (ALP), gamma-glutamyl transferase (GGT), total bilirubin, albumin, glycosylated hemoglobin (HbA1c), and lipid panel, were performed within days of the imaging studies. All samples were originally processed to serum and plasma and stored frozen at –80°C. Commercial kits were used for measurement of plasma angiotensinogen (Human Total Angiotensinogen Assay Kit – IBL; Immuno-Biological Laboratories Co. Ltd., Gunma, Japan) and the serum levels of the apoptosis-associated neo-epitope in the C-terminal domain of CK-18 (the M30-Apoptosense ELISA kit, PEVIVA; Alexis, Grünwald, Germany), complement factors C3 and C4 (turbidimetric immunoassay Tinaquant C3c and C4; Roche Diagnostics Ltd., Rotkreuz, Switzerland), glucagon (Mercodia AB, Uppsala, Sweden) and the ELF test (The ADVIA Centaur Enhanced Liver Fibrosis Test; Siemens Healthcare, Erlangen, Germany). The ELF score was produced by the ADVIA Centaur systems, by measuring the serum hyaluronic acid (HA), amino-terminal propeptide of type III procollagen (PIIINP), and tissue inhibitor of matrix metalloproteinase 1 (TIMP 1) levels as follows: ELF score= 2.278+0.851 ln(HA)+0.751 ln(P3NP)+0.394 ln(TIMP 1), where the concentration values in parentheses are in ng/mL. The body fat and lean body mass were measured using the dual-energy X-ray absorptiometry (DXA) technique (GE Healthcare, Wauwatosa, WI, USA), on the same day as the imaging studies. All patients fasted for at least 5 hours before the imaging studies, as described below. Several clinical indices and scores were calculated based on clinical and laboratory data, including the homoeostatic model assessment of insulin resistance (HOMA-IR), NAFLD fibrosis score (NFS), AST-to-platelet ratio index (APRI), and fibrosis-4 (FIB-4) index [8].

Histologic assessment

The liver biopsy was performed at the discretion of hepatologists in the hospital if indicated or systematically during bariatric surgery. After standard processing, all specimens were subjected to hematoxylin-and-eosin staining and Masson trichrome staining to assess the liver fibrosis stage. A pathologist (D.H.C.) who was blinded to the patients' clinical and radiologic results assessed the stained specimens. Histological scoring was performed using the Nonalcoholic Steatohepatitis Clinical Research Network histologic (NASH CRN) scoring system [19]. Fibrosis was staged from F0 to F4 (Supplementary Figs 1 and 2) [19].

Transient elastography

TE was performed using FibroScan 502 (Echosens, Paris, France) by a trained technician blinded to the clinical and histological data. All patients were scanned first using the M probe (3.5 MHz) or, when indicated by equipment, using the XL probe (2.5 MHz) at the right lobe of the liver. At least 10 measurements were made to obtain the median valid LSM in kilopascals (kPa) and the interquartile range (IQR). Liver steatosis values were obtained by the CAP measurement in dB/m. Technical failure was defined as no stiffness measurement obtained or unreliable measurements (defined as a success rate <60% or IQR/median >30%) [20].

MR studies

All MR examinations, including MRE, were performed with a 3-T scanner (MAGNETOM Skyra; Siemens Healthineers, Er-

langen, Germany) using an 18-channel body matrix coil and table-mounted 32-channel spine matrix coil. To quantify the liver fat content, we used a multi-echo three-dimensional gradient-echo sequence to obtain MRI-PDFF from a single breath-hold acquisition. Automated calculation and output of a stack with quantitative MRI-PDFF coding were performed and archived to the picture archiving and communication system. If the automated MRI-PDFF calculation failed, then three circular regions of interest (ROIs) were located in segment VII or VIII on the liver for each MRI-PDFF. The mean value for the three ROIs was considered the representative MRI-PDFF

High-speed T2-corrected multiecho single-voxel ^{1}H-MRS with stimulated echo acquisition mode readout was performed. Experienced MR technicians placed a spectroscopy voxel ROI (30×30×30 mm) in the superior portion of the right hepatic lobe (segment VII or VIII) with a normal appearance while avoiding large hepatic vessels, bile ducts, focal hepatic lesions, and liver margins.

The two-dimensional SE-EPI-based MRE sequence (Work-In-Progress package; Siemens Healthineers) was performed. For MRE, a cylindrical passive longitudinal pneumatic driver was attached to the right anterior chest wall using a rubber belt with the center of the driver at the level of the xiphoid process. To produce propagating shear waves in the liver, continuous longitudinal 60 Hz mechanical vibrations were used. An inversion algorithm was used to generate elastograms that depicted the shear stiffness measured in kilopascals (kPa). To obtain LSM values for the liver parenchyma, the reviewer (S.J.C., who was blinded to the patients' clinical or histologic results) drew a geographical ROI that included the largest part of the liver parenchyma (Supplementary Figs. 1 and 2) [21]. The visceral and subcutaneous fat adipose areas were calculated at the L3–L4 discs from the multi-echo three-dimensional gradient-echo sequence.

Statistical analysis

Categorical variables were compared as counts and percentages and associations were tested using the chi-square or Fisher's exact test. Continuous variables are reported as the mean±standard deviation, and differences between groups were analyzed using Student's *t*-test (two-tailed) or the Mann-Whitney *U* test as appropriate. Correlations were evaluated using the Spearman correlation coefficient. A two-tailed *P* value less than 0.05 was considered statistically significant for all analyses. Univariate and multivariate logistic regression analyses to assess for the potential predicting factors of significant liver fibrosis was performed. Characteristics determined to be statistically significant ($P<0.05$) by univariate analysis were used as input variables for multivariate logistic regression analysis. The diagnostic accuracy was assessed by the standard area under the receiver operating characteristic curve (AUROC) and the weighted AUROC. For each AUROC, 95% confidence intervals were measured using its standard error. The AUROC curves were compared according to DeLong et al. [22]. The AUROC and the Youden index were used to determine the optimal thresholds. Statistical analyses were performed using R software/environment (R-2.9.1; R Foundation for Statistical Computing, Vienna, Austria).

RESULTS

The characteristics of the study subjects

A total of 133 subjects were included in this cross-sectional study, after excluding three patients due to chronic hepatitis B ($n=2$) and C ($n=1$). Table 1 presents the characteristics of the study subjects. The mean age of the participants was 39.4 years, with a prevalence of males (46%). Of the 130 TE assessments, 82 (63%) were performed with the M probe and the XL probe was applied for 48 (37%) subjects whose BMI was at least 30 kg/m^2. Three patients failed TE (failure rate, 2.2% [3/133]).

The MR studies could not be finished in one patient due to unexpected claustrophobia. A MRE-LSM result from another patient was not included due to a disorganized wave pattern on wave images and the patient refused to receive MRE reexamination. A total of 131 patients underwent MRE. Liver biopsy data were available for 54 patients. A total of 16, 23, five, six, and four patients had fibrosis stages 0, 1, 2, 3, and 4, respectively. In the present study, the minimal diagnostic criterion for the diagnosis of NAFLD was defined as the presence of ≥5% hepatic steatosis on MRI-PDFF or NAFLD evidence based on liver biopsy, after the exclusion of secondary causes [23]. Patients with NAFLD had higher BMI, WC, and whole body and abdominal fat measured by DXA and MRI, respectively. They were more likely to have hypertension or type 2 diabetes mellitus than the non-NAFLD group. Additionally, compared with the values of the subjects without NAFLD, the NAFLD group had higher AST, ALT, HbA1c, fasting glucose, fasting insulin, glucagon, HOMA-IR, C3, C4, CK-18, low density lipoprotein cholesterol, triglycerides, and white blood cell and platelet counts in the blood tests (Table 1).

Table 1. Baseline characteristics of the study subjects

Characteristic	All subjects (n=133)	NAFLD (n=102)	No NAFLD (n=31)	P value
Age, yr	39.4±14.3	40.0±14.1	37.7±15.2	0.44
Male sex	60 (45)	41 (40)	19 (61)	<0.05
MRI-PDFF, %	13.9±10.0	17.2±9.4	3.4±0.9	<0.001
MRE-LSM, kPa	3.5±1.3	3.6±1.2	3.3±1.4	0.26
R2*, s^{-1}	54.6±16.3	59.0±15.5	42.0±6.9	<0.001
CAP, dB/m	298.0±67.2	323.4±52.6	216.9±38.3	<0.001
TE-LSM, kPa	8.4±9.3	9.4±9.5	5.1±8.0	<0.05
Weight, kg	88.7±23.5	95.5±22.2	66.3±10.3	<0.001
BMI, kg/m^2	31.7±7.6	34.3±6.7	23.2±3.2	<0.001
WC, cm	101.5±17.5	107.9±14.4	80.6±7.6	<0.001
Hypertension	33 (25)	31 (30)	2 (6)	<0.05
Type 2 diabetes mellitus	39 (29)	36 (35)	3 (10)	<0.05
AST, U/L	44.7±42.3	50.9±45.9	24.3±16.2	<0.001
ALT, U/L	60.9±69.7	72.5±75.4	22.7±17.8	<0.001
GGT, U/L	59.1±83.2	63.8±50.3	43.8±146.5	0.24
ALP, U/L	76.2±55.9	77.4±24.4	72.4±108.4	0.79
HDL-C, mg/dL	51.3±15.2	49.0±14.7	58.8±14.6	<0.05
LDL-C, mg/dL	123.1±37.8	127.9±38.3	107.4±31.5	<0.05
Triglycerides, mg/dL	145.1±94.3	154.7±84.2	113.6±117.7	<0.05
WBC, $\times 10^9$/L	6.9±2.2	7.4±2.2	5.4±1.6	<0.001
Platelet, $\times 10^9$/L	268.8±85.5	277.6±90.4	239.8±59.2	<0.05
HbA1c, %	6.3±1.7	6.6±1.8	5.5±0.8	<0.001
Glucose, mg/dL	110.6±41.2	116.3±44.8	91.5±15.2	<0.001
Insulin, μU/mL	20.9±25.6	25.4±27.8	6.7±3.9	<0.001
HOMA-IR	6.2±9.1	7.5±9.9	1.5±1.0	<0.001
Glucagon, pmol/L	12.9±8.2	14.6±8.8	8.9±4.6	<0.001
C3, mg/dL	136.6±41.0	143.1±38.1	103.8±40.6	<0.001
C4, mg/dL	31.0±10.5	31.9±10.8	26.1±6.7	<0.05
Cytokeratin-18, U/L	372.7±539.7	492.6±597.2	72.8±74.6	<0.001
Angiotensinogen, ng/mL	6.0±5.4	6.5±5.7	3.7±2.0	0.21
NFS	0.3±1.6	0.4±1.7	-0.2±1.0	<0.05
FIB-4	1.1±1.4	1.2±1.6	0.9±0.5	0.31
APRI	0.5±0.6	0.6±0.6	0.3±0.2	<0.001
ELF score	8.8±0.9	8.9±0.9	8.4±0.9	<0.05
DXA total body fat, %	39.7±12.0	43.8±9.2	26.5±10.4	<0.001
DXA total muscle, kg	44.4±18.0	44.5±18.9	44.0±14.9	0.89
MRI-visceral fat, cm^2	155.3±90.1	183.4±82.7	64.3±38.2	<0.001
MRI-subcutaneous fat, cm^2	261.2±133.1	302.1±122.7	129.3±59.0	<0.001

Values are presented as mean±standard deviation or number (%).
NAFLD, nonalcoholic fatty liver disease; MRI-PDFF, magnetic resonance imaging-estimated proton density fat fraction; MRE, magnetic resonance elastography; LSM, liver stiffness measurement; R2*, R2* relaxation rate; CAP, controlled attenuation parameter; TE, transient elastography; BMI, body mass index; WC, waist circumference; AST, aspartate aminotransferase; ALT, alanine aminotransferase; GGT, gamma-glutamyl transpeptidase; ALP, alkaline phosphatase; HDL-C, high density lipoprotein cholesterol; LDL-C, low density lipoprotein cholesterol; WBC, white blood cell; HbA1c, glycosylated hemoglobin; HOMA-IR, homoeostatic model assessment of insulin resistance; C3, complement component 3; C4, complement component 4; NFS, nonalcoholic fatty liver disease fibrosis score; FIB-4, fibrosis-4; APRI, AST-to-platelet ratio index; ELF, enhanced liver fibrosis; DXA, dual-energy X-ray absorptiometry.

Evaluation of hepatic steatosis and its association with various parameters

For the evaluation of hepatic steatosis, the MRI-PDFF study was performed in the same session as the ^{1}H-MRS examination and on the same day or within 1 or 2 days of the TE examination. The MRI-PDFF correlated perfectly with the ^{1}H-MRS, whereas the TE-CAP showed only a modest correlation with the ^{1}H-MRS or MRI-PDFF (Fig. 1). Compared with those of the TE-CAP, the MRI-PDFF showed better correlations with fasting circulating AST, ALT, glucose, glucagon, triglycerides, C3, and CK-18 levels as well as the HOMA-IR value (Table 2). However, the TE-CAP showed higher correlations with BMI, WC, DXA total body fat (%), and MRI-measured abdominal fat areas than the MRI-PDFF (Table 2).

The optimal cutoff values of TE-CAP and ALT for the prediction of hepatic steatosis (≥5% on MRI-PDFF) were 264 dB/m and 31 U/L, respectively (Fig. 2). When the upper limits of normal for ALT were defined as 35 and 25 U/L for the male and female subjects, respectively [24], the optimal discriminating cutoff values of MRI-PDFF and TE-CAP for abnormal ALT were 9.9% and 270 dB/m, respectively, with a higher AUROC with MRI-PDFF (Fig. 2).

Evaluation of hepatic fibrosis and related factors

The MRE-LSM showed significant correlations with the blood AST, ALT, GGT, ALP, and CK-18 levels; the platelet count (negative); and the clinical and ELF scores, whereas the TE-LSM showed poor or weak correlations with those parameters (Table 3, Fig. 1).

Both MRE- and TE-measured LSM values showed a higher correlation with the APRI and FIB-4 index than with the NFS (Table 3). The NFS, FIB-4 index, and APRI scores were categorized using their respective lower and higher cutoff values, which have been suggested for the exclusion or prediction of advanced fibrosis (for the NFS <−1.455 and >0.676; for the FIB-4 index <1.3 and >2.67; and for the APRI <0.5 and >1.5, respectively) [8]. There was less overlap in both the MRE-LSM and TE-LSM values between the low-, intermediate-, and high-risk fibrosis groups based on the FIB-4 index than in those groups based on the NFS or APRI (Supplementary Fig. 3).

When we analyzed liver-biopsied patients (n=54), the MRE, TE and the ELF score showed statistical significance in differentiating significant fibrosis (≥F2) from no or minimal hepatic fibrosis (F0/1). However, the ELF score showed more overlap between the fibrosis grades and wider variation within each fi-

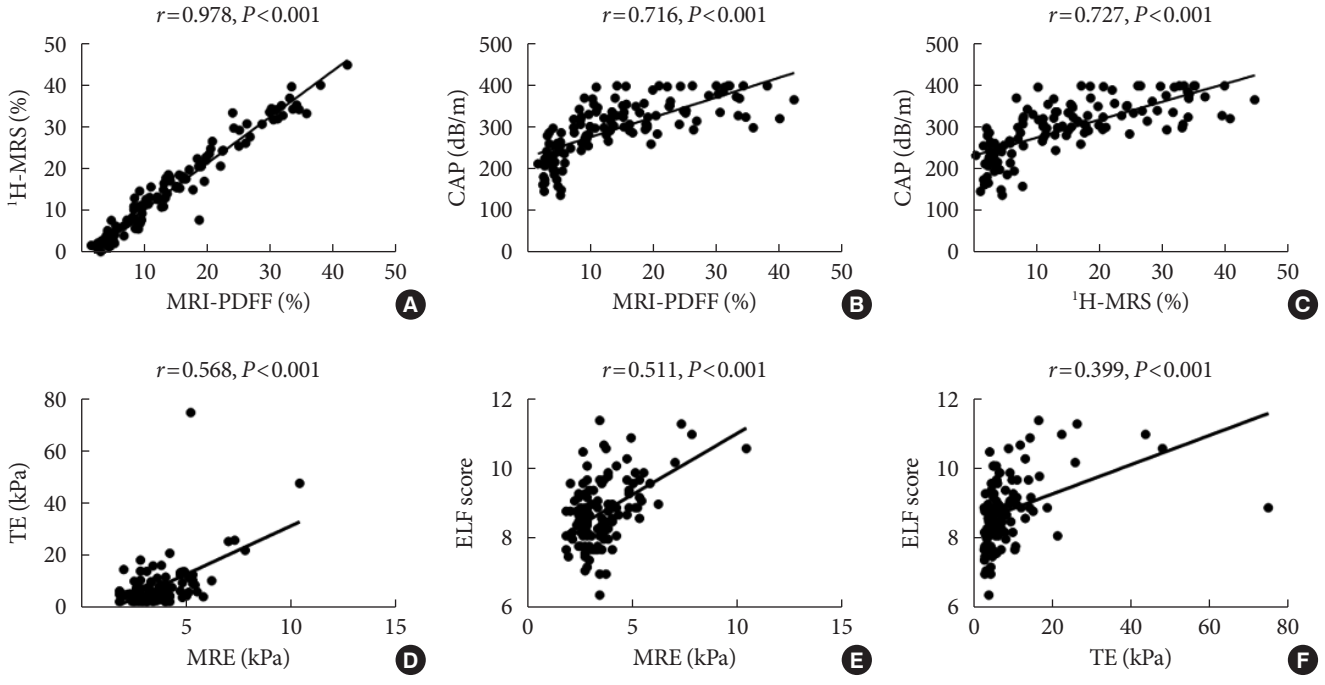

Fig. 1. Correlations between magnetic resonance-based and transient elastography (TE)-based parameters for the assessment of steatosis (A, B, C) and among magnetic resonance elastography (MRE)-liver stiffness measurement (LSM), TE-LSM, and the enhanced liver fibrosis (ELF) score for the assessment of hepatic fibrosis (D, E, F). ^{1}H-MRS, magnetic resonance spectroscopy; CAP, controlled attenuation parameter; MRI-PDFF, magnetic resonance imaging-estimated proton density fat fraction.

Table 2. The relationships of MRI-PDFF and TE-CAP with other factors

Parameter	Correlation coefficient (*r*)	95% CI	*P* value
MRI-PDFF correlates with			
^{1}H-MRS, %	0.978	0.970 to 0.985	<0.001
R2*, s^{-1}	0.822	0.757 to 0.870	<0.001
CAP, dB/m	0.716	0.620 to 0.791	<0.001
Age, yr	–0.194	–0.353 to –0.024	<0.05
Weight, kg	0.598	0.476 to 0.698	<0.001
BMI, kg/m^2	0.618	0.500 to 0.713	<0.001
WC, cm	0.590	0.466 to 0.691	<0.001
DXA total body fat, %	0.532	0.396 to 0.645	<0.001
DXA total muscle, kg	0.069	–0.104 to 0.238	0.43
MRI-visceral fat, cm^2	0.492	0.350 to 0.612	<0.001
MRI-subcutaneous fat, cm^2	0.596	0.473 to 0.696	<0.001
AST, U/L	0.347	0.187 to 0.488	<0.001
ALT, U/L	0.376	0.219 to 0.513	<0.001
GGT, U/L	0.140	–0.031 to 0.303	0.10
Triglycerides, mg/dL	0.273	0.107 to 0.424	<0.05
HbA1c, %	0.297	0.133 to 0.445	<0.001
Fasting glucose, mmol/L	0.280	0.115 to 0.430	<0.05
Insulin, μU/mL	0.363	0.203 to 0.503	<0.001
Glucagon, pmol/L	0.381	0.158 to 0.566	<0.05
HOMA-IR	0.339	0.176 to 0.483	<0.001
C3, mg/dL	0.486	0.333 to 0.614	<0.001
Cytokeratin-18, U/L	0.593	0.414 to 0.727	<0.001
Angiotensinogen, ng/mL	–0.008	–0.308 to 0.292	0.95
TE-CAP correlates with			
^{1}H-MRS, %	0.727	0.633 to 0.799	<0.001
R2*, s^{-1}	0.580	0.453 to 0.685	<0.001
Age, yr	0.048	–0.125 to 0.218	0.58
Weight, kg	0.639	0.524 to 0.730	<0.001
BMI, kg/m^2	0.733	0.642 to 0.804	<0.001
WC, cm	0.716	0.621 to 0.791	<0.001
DXA total body fat, %	0.662	0.552 to 0.749	<0.001
DXA total muscle, kg	0.015	–0.158 to 0.188	0.86
MRI-visceral fat, cm^2	0.609	0.487 to 0.708	<0.001
MRI-subcutaneous fat, cm^2	0.674	0.566 to 0.758	<0.001
AST, U/L	0.157	–0.014 to 0.321	0.07
ALT, U/L	0.217	0.046 to 0.375	<0.05
GGT, U/L	0.094	–0.080 to 0.262	0.28
Triglycerides, mg/dL	0.236	0.066 to 0.393	<0.05
HbA1c, %	0.301	0.135 to 0.450	<0.001
Fasting glucose, mmol/L	0.221	0.050 to 0.378	<0.05

(*Continued to the next page*)

Table 2. Continued

Parameter	Correlation coefficient (*r*)	95% CI	*P* value
Insulin, μU/mL	0.281	0.113 to 0.434	<0.05
Glucagon, pmol/L	0.333	0.106 to 0.526	<0.05
HOMA-IR	0.253	0.082 to 0.410	<0.05
C3, mg/dL	0.332	0.157 to 0.487	<0.001
Cytokeratin-18, U/L	0.319	0.090 to 0.515	<0.05
Angiotensinogen, ng/mL	0.297	0.0001 to 0.545	0.05

MRI-PDFF, magnetic resonance imaging-estimated proton density fat fraction; TE, transient elastography; CAP, controlled attenuation parameter; CI, confidence interval; ^{1}H-MRS, proton magnetic resonance spectroscopy; R2*, R2* relaxation rate; BMI, body mass index; WC, waist circumference; DXA, dual-energy X-ray absorptiometry; AST, aspartate aminotransferase; ALT, alanine aminotransferase; GGT, gamma-glutamyl transpeptidase; HbA1c, glycosylated hemoglobin; HOMA-IR, homoeostatic model assessment of insulin resistance; C3, complement component 3.

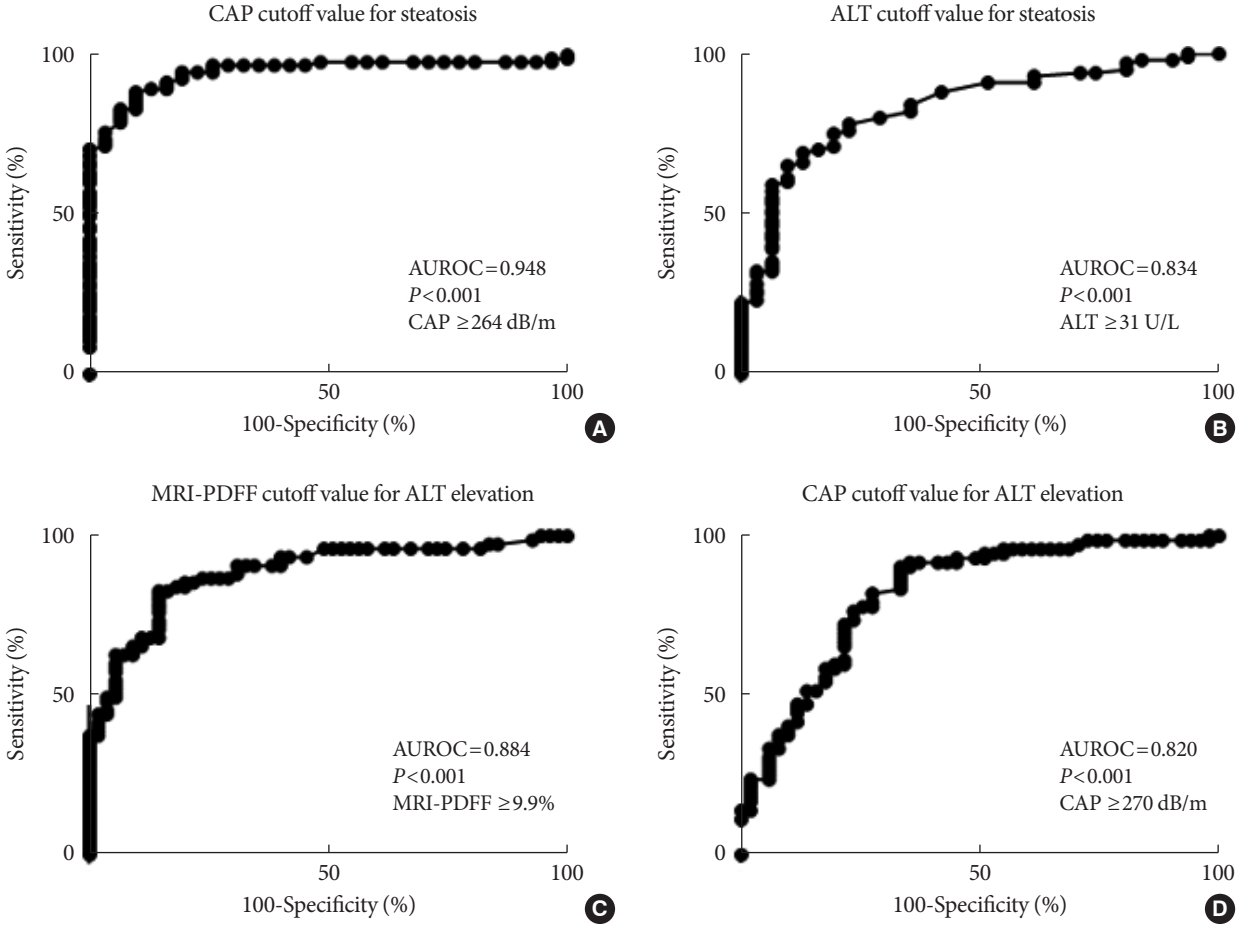

Fig. 2. Determination of the areas under the receiver operating characteristic curves (AUROCs) for the cutoff levels of transient elastography (TE)-controlled attenuation parameter (CAP) for steatosis definition and of the liver fat level associated with an abnormal alanine aminotransferase (ALT) value. The upper limits of normal for ALT (i.e., 35 and 25 U/L for males and females, respectively) were defined based on a recent guidance [24]. (A) TE-CAP cutoff value corresponding to magnetic resonance imaging-estimated proton density fat fraction (MRI-PDFF) 5% or more. (B) ALT cutoff value corresponding to MRI-PDFF 5% or more. (C) MRI-PDFF cutoff level corresponding to the upper limit of normal for ALT. (D) TE-CAP cutoff value corresponding to the upper limit of normal for ALT.

Table 3. The relationships of MRE-LSM and TE-LSM with other factors

Parameter	Correlation coefficient (*r*)	95% CI	*P* value
MRE-LSM correlates with			
Age, yr	0.244	0.075 to 0.399	<0.05
Weight, kg	0.084	−0.088 to 0.252	0.33
BMI, kg/m^2	0.028	−0.144 to 0.198	0.75
WC, cm	0.115	−0.057 to 0.281	0.18
DXA total body fat, %	−0.033	−0.205 to 0.140	0.70
DXA total muscle, kg	−0.133	−0.299 to 0.399	0.13
MRI-visceral fat, cm^2	0.264	0.096 to 0.417	<0.05
MRI-subcutaneous fat, cm^2	−0.005	−0.177 to 0.166	0.95
R2*, s^{-1}	−0.053	−0.223 to 0.117	0.54
TE-LSM, kPa	0.568	0.437 to 0.675	<0.001
AST, U/L	0.352	0.192 to 0.494	<0.001
ALT, U/L	0.264	0.097 to 0.417	<0.05
GGT, U/L	0.631	0.515 to 0.724	<0.001
ALP, U/L	0.543	0.410 to 0.654	<0.001
WBC, ×10^9/L	0.016	−0.156 to 0.186	0.85
Platelet, ×10^9/L	−0.323	−0.468 to −0.160	<0.001
HOMA-IR	−0.040	−0.213 to 0.133	0.65
C3, mg/dL	0.201	0.018 to 0.371	<0.05
Cytokeratin-18, U/L	0.477	0.270 to 0.641	<0.001
Angiotensinogen, ng/mL	0.132	−0.174 to 0.416	0.39
NFS	0.444	0.295 to 0.572	<0.001
FIB-4	0.491	0.348 to 0.611	<0.001
APRI	0.523	0.386 to 0.637	<0.001
ELF score	0.511	0.368 to 0.630	<0.001
TE-LSM correlates with			
Age, yr	0.083	−0.090 to 0.251	<0.001
Weight, kg	0.393	0.236 to 0.529	<0.001
BMI, kg/m^2	0.374	0.215 to 0.513	<0.001
WC, cm	0.428	0.276 to 0.559	<0.001
DXA total body fat, %	0.195	0.022 to 0.356	<0.05
DXA total muscle, kg	0.069	−0.105 to 0.239	0.43
MRI-visceral fat, cm^2	0.376	0.217 to 0.516	<0.001
MRI-subcutaneous fat, cm^2	0.296	0.129 to 0.447	<0.001
R2*, s^{-1}	0.072	−0.102 to 0.242	0.41
AST, U/L	0.187	0.016 to 0.348	<0.05
ALT, U/L	0.130	−0.042 to 0.296	0.14
GGT, U/L	0.565	0.434 to 0.672	<0.001
ALP, U/L	0.437	0.286 to 0.566	<0.001
WBC, ×10^9/L	0.239	0.069 to 0.394	<0.05

(*Continued to the next page*)

Table 3. Continued

Parameter	Correlation coefficient (*r*)	95% CI	*P* value
Platelet, $\times 10^9$/L	−0.153	−0.317 to 0.019	0.08
HOMA-IR	0.078	−0.097 to 0.250	0.38
C3, mg/dL	0.259	0.078 to 0.423	<0.05
Cytokeratin-18, U/L	0.214	−0.021 to 0.427	0.07
Angiotensinogen, ng/mL	0.285	−0.012 to 0.537	0.06
NFS	0.263	0.094 to 0.417	<0.05
FIB-4	0.287	0.120 to 0.438	<0.05
APRI	0.295	0.129 to 0.445	<0.001
ELF score	0.399	0.239 to 0.538	<0.001

MRE, magnetic resonance elastography; LSM, liver stiffness measurement; TE, transient elastography; CI, confidence interval; BMI, body mass index; WC, waist circumference; DXA, dual-energy X-ray absorptiometry; MRI, magnetic resonance imaging; R2*, R2* relaxation rate; AST, aspartate aminotransferase; ALT, alanine aminotransferase; GGT, gamma-glutamyl transpeptidase; ALP, alkaline phosphatase; WBC, white blood cell; HOMA-IR, homoeostatic model assessment of insulin resistance; C3, complement component 3; NFS, nonalcoholic fatty liver disease fibrosis score; FIB-4, fibrosis-4; APRI, AST-to-platelet ratio index; ELF, enhanced liver fibrosis.

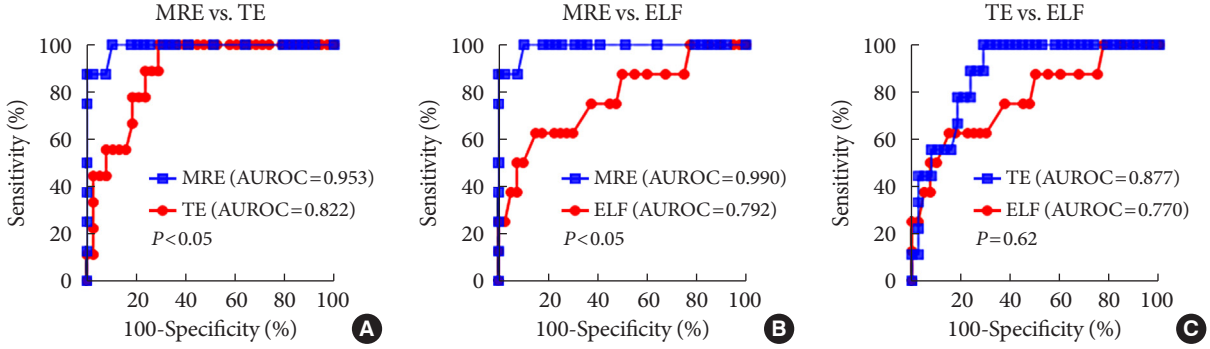

Fig. 3. Comparisons of the areas under the receiver operating characteristic curves (AUROCs) for magnetic resonance elastography (MRE), transient elastography (TE), and the enhanced liver fibrosis (ELF) test for a diagnosis of advanced fibrosis (≥F3) in the biopsied subjects (n=54). (A) The comparison of the AUROC between MRE and TE, (B) the comparison of the AUROC between MRE and ELF test, and (C) the comparison of the AUROC between TE and ELF test.

brosis grade than the MRE- or TE-LSM (Supplementary Fig. 4). In addition, MRE performed better in differentiating advanced fibrosis (≥F3) from lower grade hepatic fibrosis (<F3) than TE and the ELF test (Fig. 3). The cutoff values for advanced fibrosis were 3.9 kPa for MRE-LSM, 8.1 kPa for TE-LSM and 9.2 for the ELF test.

When we analyzed liver-biopsied patients (n=54), the optimal discriminating cutoff value of significant fibrosis (≥F2) based on MRE from those with lower grade fibrosis (<F2) was 3.8 kPa. We dichotomized the subjects between significant fibrosis and non-significant fibrosis groups by utilizing this cutoff value (3.8 kPa) (Supplementary Table 1). Based on this cutoff value, patients with high MRE-LSM (≥3.8 kPa) had higher age and other various unfavorable body and metabolic parameters, and lower platelet count compared to those who represented low MRE-LSM (<3.8 kPa). Factors associated with high MRE-LSM on univariate analysis were age, type 2 diabetes mellitus, AST, ALT, GGT, ALP, platelet count, MRI-PDFF, and MRI-visceral and subcutaneous fat areas. Multivariate analyses showed that age (odds ratio [OR], 1.058; P<0.05), ALP (OR, 1.023; P<0.05), and platelet count (OR, 0.990; P<0.05) were found the potential predictors for significant fibrosis based on the MRE-LSM cutoff value (Supplementary Table 2).

DISCUSSION

NAFLD is among the most common metabolic disorders with a broad spectrum of disease entities and requires widely avail-

able and relatively exact diagnostic tools for the diagnosis and assessment of its specific disease stages [2,25]. Although hepatic fibrosis is the most important and independent prognostic factor in NAFLD [5,6], liver biopsy, which is the gold standard for fibrosis staging in NAFLD, is not performed for the majority of patients with NAFLD. As alternatives, noninvasive tools for the assessment of NAFLD have received much attention, and some noninvasive methods have been validated and are available in a clinical-dependent context [26].

In the present study, we aimed to evaluate whether MR-based examinations better reflected the pathophysiologic features and fibrosis progression in NAFLD and to compare the methods with other noninvasive tools in the differentiation of advanced fibrosis, including clinical scoring systems, the ELF test, and TE. Few studies have tried to correlate pathophysiologic and metabolic features with the results of these three validated noninvasive examinations simultaneously [16].

Our results revealed that the MRI-PDFF correlated perfectly with the liver fat measured by ^{1}H-MRS and had a significant association with other various pathophysiologic and metabolic parameters including liver enzyme activities, lipid and glucose metabolism, insulin resistance, the marker of hepatocyte apoptosis (CK-18), and inflammation (C3). In contrast, the TE-CAP correlated more with BMI than with the ^{1}H-MRS-measured liver fat and showed a closer association with body fat, abdominal subcutaneous fat, and WC than with the above-mentioned pathophysiologic parameters. The reason that the TE-CAP correlated more with anthropometric than with metabolic parameters seems to be related to the principle of the CAP, which measures total ultrasonic attenuation [27]. Because obesity is associated with a higher skin-to-liver capsule distance due to subcutaneous fat, the presence of thicker non-hepatic tissue between the liver and the TE probe has been shown to significantly affect the CAP values [27]. In the present study, the cutoff level of the TE-CAP value corresponding to MRI-PDFF ≥5% was 264 dB/m. To define steatosis, variable cutoff levels of the TE-CAP value have been reported, ranging from 243 to 288 dB/m [20,28]. In addition, a previous study showed that an increased TE-CAP value was also associated with an overestimation of LSM by TE, especially in patients with lower fibrosis stages [29]. Thus, in obese patients, TE can increase the false positive LSM results for advanced fibrosis, as the TE-CAP increases with its known failure rate and there is a significant rate of disagreement between repeated examinations [30]. Collectively, our results suggest that MRI-PDFF is an accurate and reproducible noninvasive tool that removes the technical complexity of the ^{1}H-MRS protocol and is not affected by patient factors (e.g., BMI and subcutaneous fat), which are important confounding factors for TE examination.

The degree of steatosis related to early ALT elevation during the course of NAFLD has not been studied extensively. However, this issue seems to be important, because a significant proportion of patients with NAFLD have a normal ALT level [31]. Our results showed that the hepatic fat cutoff level associated with an abnormal ALT level were 9.9%. This PDFF value is lower than the previously reported NASH-predicting PDFF value (i.e., 12.4%) [32]. However, it is of note that in some patients with NAFLD and normal liver enzymes, hepatic fibrosis also needs to be tested [33]. The clinical implications of those PDFF cutoff values in NAFLD need to be studied further with other noninvasive tools for the discrimination of NASH and/or fibrosis from simple steatosis.

Regarding the hepatic fibrosis assessment in the present study, MRE-LSM better correlated with the clinical and ELF scores and other pathophysiologically relevant parameters than TE-LSM. And, MRE outperformed both TE and the ELF test in discriminating advanced fibrosis in NAFLD. The excellent performance of MRE in this study echoed previous studies [13,18,34]. However, few studies have evaluated MRE simultaneously with TE, the ELF and clinical scores, and serum biomarkers [16]. Collectively, the comprehensive analysis of noninvasive tools for assessing hepatic fibrosis in the present study showed that MRE performed better than other tools in both mechanical and pathophysiologic aspects. TE-LSM showed marginal significance in differentiating significant fibrosis, whereas the ELF score did not. However, TE did not outperform the ELF test in differentiating advanced fibrosis. In the present study, the cutoff values for advanced fibrosis were 3.9 kPa for MRE-LSM, 8.1 kPa for TE-LSM, and for 9.2 for the ELF test. These values are in the ranges of previous reports [16,35-37].

Additionally, many indirect clinical scoring systems for the assessment of fibrosis, including the NFS, FIB-4 index, and APRI, and direct serum markers for extracellular matrix turnover, including the ELF test, have been studied frequently [8]. The NFS, FIB-4 index, and APRI may perform relatively well in excluding or predicting advanced fibrosis with their respective lower and higher cutoff values [8]. Each of the three groups categorized by applying the low and high risk for fibrosis cutoff values of the three clinical scoring systems did show signifi-

cantly overlapping MRE- and TE-LSM values, especially for NFS, but less so with the FIB-4 index. In addition, APRI and FIB-4 correlated better with MRE-LSM than NFS in the present study. Thus, in line with a previous study [38], our results suggest that FIB-4 better discriminates fibrosis stages than the other two scoring systems. The ELF score may be a useful blood test for the exclusion of fibrosis by applying a cutoff value of 7.7 and can significantly discriminate cirrhosis by applying a higher cutoff value (e.g., 11.3) [39]. However, cautious interpretation is required because age (increased with age) and sex (lower in females) also significantly affect the ELF score.

In addition, the CK-18 M30 fragment, which is a marker of hepatocyte apoptosis [8], was increased and correlated better with the MR-based parameters than with the TE parameters. Furthermore, the level of the M30 fragment correlated well with C3 (r=0.423, P<0.001, data not shown), which was reported to be associated with excessive fat accumulation, hepatocyte apoptosis, and hepatic neutrophil sequestration and to play a role in NAFLD progression [40]. Unfortunately, we could not include the C-reactive protein levels in the analysis due to missing values in the majority of cases. Our results showed that the MR-based parameters better matched both hepatocyte apoptosis and necroinflammation, which was in line with the results of a previous study in which longitudinal changes in the CK-18 M30 fragment and PDFF were correlated with each other after medical treatment [16].

Our results show that although TE may be a reasonable initial option to evaluate patients with NAFLD and to exclude or differentiate advanced hepatic fibrosis, MR-based protocols, which have undergone rapid technical development, are becoming user-friendly and better capture the pathophysiologic, histologic, and metabolic features of NAFLD. In line with our view, MRI-PDFF and MRE have been shown to outperform TE in discriminating the progression of hepatic steatosis and fibrosis [13,34].

The strengths of the current study include the comprehensive analyses of various noninvasive assessment tools for NAFLD. In addition, we included not only liver fat and LSM values but also various pathophysiologic parameters in the analysis, which supported the superiority of the MR-based techniques compared to those of the other methods in various aspects. This study also has several limitations. First, a liver biopsy was performed in a relatively small number of participants. However, in the case of steatosis, MRI-PDFF can measure liver fat more precisely than biopsy [7,20]. Additionally, LSM measured by MRE may reflect a larger area of liver pathology than that covered by TE or biopsy, which may suffer from sampling variability. Second, this study has a cross-sectional design. Longitudinal follow-up data and therapeutic responses need to be included in future studies. Third, the present study was performed in a single center, which may not represent the Korean population.

In conclusion, when we compared several noninvasive methods to assess NAFLD, including MRI-based methods, TE, the ELF score, other serum markers and clinical scoring systems, we found that MRI-based techniques (MRI-PDFF and MRE) were the best at measuring steatosis accurately, discriminating advanced hepatic fibrosis, and capturing pathophysiologic and metabolic features of the disease.

SUPPLEMENTARY MATERIALS

Supplementary materials related to this article can be found online at https://doi.org/10.4093/dmj.2020.0137.

CONFLICTS OF INTEREST

No potential conflict of interest relevant to this article was reported.

AUTHOR CONTRIBUTIONS

Conception or design: D.H.L.
Acquisition, analysis, or interpretation of data: S.J.C., S.M.K., Y.S.K., O.S.K., S.K.S., K.K.K., K.L., I.B.P., C.S.C., D.H.C., J.J., M.Y.P., D.H.L.
Drafting the work or revising: S.J.C., D.H.L.
Final approval of the manuscript: S.J.C., S.M.K., Y.S.K., O.S.K., S.K.S., K.K.K., K.L., I.B.P., C.S.C., D.H.C., J.J., M.Y.P., D.H.L.

ORCID

Seung Joon Choi *https://orcid.org/0000-0003-3861-7682*
Seong Min Kim *https://orcid.org/0000-0002-6453-5253*
Dae Ho Lee *https://orcid.org/0000-0002-8832-3052*

FUNDING

This study was funded by the Ministry of Health & Welfare, Korea (HI14C1135).

ACKNOWLEDGMENTS

This study was supported by a grant from the Korea Health Technology R&D Project through the Korea Health Industry Development Institute (KHIDI).

REFERENCES

1. Younossi ZM, Koenig AB, Abdelatif D, Fazel Y, Henry L, Wymer M. Global epidemiology of nonalcoholic fatty liver disease-Meta-analytic assessment of prevalence, incidence, and outcomes. Hepatology 2016;64:73-84.
2. Lee YH, Cho Y, Lee BW, Park CY, Lee DH, Cha BS, et al. Nonalcoholic fatty liver disease in diabetes. Part I: epidemiology and diagnosis. Diabetes Metab J 2019;43:31-45.
3. Portillo-Sanchez P, Bril F, Maximos M, Lomonaco R, Biernacki D, Orsak B, et al. High prevalence of nonalcoholic fatty liver disease in patients with type 2 diabetes mellitus and normal plasma aminotransferase levels. J Clin Endocrinol Metab 2015; 100:2231-8.
4. Musso G, Gambino R, Cassader M, Pagano G. Meta-analysis: natural history of non-alcoholic fatty liver disease (NAFLD) and diagnostic accuracy of non-invasive tests for liver disease severity. Ann Med 2011;43:617-49.
5. Ekstedt M, Hagstrom H, Nasr P, Fredrikson M, Stal P, Kechagias S, et al. Fibrosis stage is the strongest predictor for disease-specific mortality in NAFLD after up to 33 years of follow-up. Hepatology 2015;61:1547-54.
6. Angulo P, Kleiner DE, Dam-Larsen S, Adams LA, Bjornsson ES, Charatcharoenwitthaya P, et al. Liver fibrosis, but no other histologic features, is associated with long-term outcomes of patients with nonalcoholic fatty liver disease. Gastroenterology 2015;149:389-97.
7. Bannas P, Kramer H, Hernando D, Agni R, Cunningham AM, Mandal R, et al. Quantitative magnetic resonance imaging of hepatic steatosis: Validation in ex vivo human livers. Hepatology 2015;62:1444-55.
8. Castera L. Noninvasive evaluation of nonalcoholic fatty liver disease. Semin Liver Dis 2015;35:291-303.
9. Wong VW, Vergniol J, Wong GL, Foucher J, Chan HL, Le Bail B, et al. Diagnosis of fibrosis and cirrhosis using liver stiffness measurement in nonalcoholic fatty liver disease. Hepatology 2010;51:454-62.
10. de Ledinghen V, Vergniol J, Capdepont M, Chermak F, Hiriart JB, Cassinotto C, et al. Controlled attenuation parameter (CAP) for the diagnosis of steatosis: a prospective study of 5323 examinations. J Hepatol 2014;60:1026-31.
11. Dulai PS, Sirlin CB, Loomba R. MRI and MRE for non-invasive quantitative assessment of hepatic steatosis and fibrosis in NAFLD and NASH: clinical trials to clinical practice. J Hepatol 2016;65:1006-16.
12. Shi Y, Xia F, Li QJ, Li JH, Yu B, Li Y, et al. Magnetic resonance elastography for the evaluation of liver fibrosis in chronic hepatitis B and C by using both gradient-recalled echo and spin-echo echo planar imaging: a prospective study. Am J Gastroenterol 2016;111:823-33.
13. Park CC, Nguyen P, Hernandez C, Bettencourt R, Ramirez K, Fortney L, et al. Magnetic resonance elastography vs transient elastography in detection of fibrosis and noninvasive measurement of steatosis in patients with biopsy-proven nonalcoholic fatty liver disease. Gastroenterology 2017;152:598-607.
14. Loomba R, Sirlin CB, Ang B, Bettencourt R, Jain R, Salotti J, et al. Ezetimibe for the treatment of nonalcoholic steatohepatitis: assessment by novel magnetic resonance imaging and magnetic resonance elastography in a randomized trial (MOZART trial). Hepatology 2015;61:1239-50.
15. Le TA, Chen J, Changchien C, Peterson MR, Kono Y, Patton H, et al. Effect of colesevelam on liver fat quantified by magnetic resonance in nonalcoholic steatohepatitis: a randomized controlled trial. Hepatology 2012;56:922-32.
16. Jayakumar S, Middleton MS, Lawitz EJ, Mantry PS, Caldwell SH, Arnold H, et al. Longitudinal correlations between MRE, MRI-PDFF, and liver histology in patients with non-alcoholic steatohepatitis: analysis of data from a phase II trial of selonsertib. J Hepatol 2019;70:133-41.
17. Guha IN, Parkes J, Roderick P, Chattopadhyay D, Cross R, Harris S, et al. Noninvasive markers of fibrosis in nonalcoholic fatty liver disease: validating the European Liver Fibrosis Panel and exploring simple markers. Hepatology 2008;47:455-60.
18. Huwart L, Sempoux C, Vicaut E, Salameh N, Annet L, Danse E, et al. Magnetic resonance elastography for the noninvasive staging of liver fibrosis. Gastroenterology 2008;135:32-40.
19. Kleiner DE, Brunt EM, Van Natta M, Behling C, Contos MJ, Cummings OW, et al. Design and validation of a histological scoring system for nonalcoholic fatty liver disease. Hepatology 2005;41:1313-21.
20. Caussy C, Alquiraish MH, Nguyen P, Hernandez C, Cepin S, Fortney LE, et al. Optimal threshold of controlled attenuation parameter with MRI-PDFF as the gold standard for the detection of hepatic steatosis. Hepatology 2018;67:1348-59.

21. Venkatesh SK, Yin M, Ehman RL. Magnetic resonance elastography of liver: technique, analysis, and clinical applications. J Magn Reson Imaging 2013;37:544-55.
22. DeLong ER, DeLong DM, Clarke-Pearson DL. Comparing the areas under two or more correlated receiver operating characteristic curves: a nonparametric approach. Biometrics 1988;44:837-45.
23. Chalasani N, Younossi Z, Lavine JE, Charlton M, Cusi K, Rinella M, et al. The diagnosis and management of nonalcoholic fatty liver disease: practice guidance from the American Association for the Study of Liver Diseases. Hepatology 2018;67:328-57.
24. Terrault NA, Lok ASF, McMahon BJ, Chang KM, Hwang JP, Jonas MM, et al. Update on prevention, diagnosis, and treatment of chronic hepatitis B: AASLD 2018 hepatitis B guidance. Hepatology 2018;67:1560-99.
25. Newsome PN, Cramb R, Davison SM, Dillon JF, Foulerton M, Godfrey EM, et al. Guidelines on the management of abnormal liver blood tests. Gut 2018;67:6-19.
26. Younossi ZM, Loomba R, Anstee QM, Rinella ME, Bugianesi E, Marchesini G, et al. Diagnostic modalities for nonalcoholic fatty liver disease, nonalcoholic steatohepatitis, and associated fibrosis. Hepatology 2018;68:349-60.
27. Shen F, Zheng RD, Shi JP, Mi YQ, Chen GF, Hu X, et al. Impact of skin capsular distance on the performance of controlled attenuation parameter in patients with chronic liver disease. Liver Int 2015;35:2392-400.
28. Karlas T, Petroff D, Sasso M, Fan JG, Mi YQ, de Ledinghen V, et al. Individual patient data meta-analysis of controlled attenuation parameter (CAP) technology for assessing steatosis. J Hepatol 2017;66:1022-30.
29. Petta S, Wong VW, Camma C, Hiriart JB, Wong GL, Marra F, et al. Improved noninvasive prediction of liver fibrosis by liver stiffness measurement in patients with nonalcoholic fatty liver disease accounting for controlled attenuation parameter values. Hepatology 2017;65:1145-55.
30. Vuppalanchi R, Siddiqui MS, Van Natta ML, Hallinan E, Brandman D, Kowdley K, et al. Performance characteristics of vibration-controlled transient elastography for evaluation of nonalcoholic fatty liver disease. Hepatology 2018;67:134-44.
31. Kotronen A, Westerbacka J, Bergholm R, Pietilainen KH, Yki-Jarvinen H. Liver fat in the metabolic syndrome. J Clin Endocrinol Metab 2007;92:3490-7.
32. Wildman-Tobriner B, Middleton MM, Moylan CA, Rossi S, Flores O, Chang ZA, et al. Association between magnetic resonance imaging-proton density fat fraction and liver histology features in patients with nonalcoholic fatty liver disease or nonalcoholic steatohepatitis. Gastroenterology 2018;155:1428-35.
33. Yki-Jarvinen H. Diagnosis of non-alcoholic fatty liver disease (NAFLD). Diabetologia 2016;59:1104-11.
34. Imajo K, Kessoku T, Honda Y, Tomeno W, Ogawa Y, Mawatari H, et al. Magnetic resonance imaging more accurately classifies steatosis and fibrosis in patients with nonalcoholic fatty liver disease than transient elastography. Gastroenterology 2016;150:626-37.
35. Castera L, Friedrich-Rust M, Loomba R. Noninvasive assessment of liver disease in patients with nonalcoholic fatty liver disease. Gastroenterology 2019;156:1264-81.
36. Vilar-Gomez E, Chalasani N. Non-invasive assessment of non-alcoholic fatty liver disease: clinical prediction rules and blood-based biomarkers. J Hepatol 2018;68:305-15.
37. Mikolasevic I, Orlic L, Franjic N, Hauser G, Stimac D, Milic S. Transient elastography (FibroScan(®)) with controlled attenuation parameter in the assessment of liver steatosis and fibrosis in patients with nonalcoholic fatty liver disease: where do we stand? World J Gastroenterol 2016;22:7236-51.
38. McPherson S, Stewart SF, Henderson E, Burt AD, Day CP. Simple non-invasive fibrosis scoring systems can reliably exclude advanced fibrosis in patients with non-alcoholic fatty liver disease. Gut 2010;59:1265-9.
39. Lichtinghagen R, Pietsch D, Bantel H, Manns MP, Brand K, Bahr MJ. The Enhanced Liver Fibrosis (ELF) score: normal values, influence factors and proposed cut-off values. J Hepatol 2013;59:236-42.
40. Rensen SS, Slaats Y, Driessen A, Peutz-Kootstra CJ, Nijhuis J, Steffensen R, et al. Activation of the complement system in human nonalcoholic fatty liver disease. Hepatology 2009;50:1809-17.